Available online at www.sciencedirect.com
ScienceDirect
Computers and Structures 84 (2006) 2151–2158
Computers & Structures
www.elsevier.com/locate/compstruc

Eight-node quadrilateral double-curved surface element for membrane analysis

Dezső Hegyi [a,*], István Sajtos [a], György Geiszter [b], Krisztián Hincz [c]

[a] Budapest University of Technology and Economics (BUTE), H-1111 Budapest, Műegyetem rkp. 3, Hungary
[b] H-1021 Sopron, Juharfa u. 2, Hungary
[c] HAS-BUTE Research Group for Computational Structural Mechanics, H-1111 Budapest, Műegyetem rkp. 3, Hungary

Received 23 November 2005; accepted 7 August 2006
Available online 25 October 2006

Abstract

The dynamic relaxation method is applied to membrane analysis using an eight-node quadrilateral element. The element uses second order shape functions to approximate the geometry of the structure. The element is based on the element of Gosling and Lewis [Gosling PD, Lewis WJ. Optimal structural membranes—I. Formulation of a curved quadrilateral element for surface definition. Comp Struct 1996;61:871–83]. They used a finite element approach. In this paper exact tensorial calculation is used to determine the exact deformation between the deformation-free state and the actual state.

Keywords: Dynamic relaxation method; Nonlinear continuum mechanics; Curved membrane element

1. Introduction

The dynamic relaxation method (DRM) is a suitable method for nonlinear analysis. The membrane structures are highly nonlinear, since both the geometry and the material properties of these structures are nonlinear, therefore DRM is frequently used to analyse the membrane structures. In this paper only the geometrical nonlinearity is taken into consideration.

Triangle, three-node elements are used to describe the surface of the double-curved membrane structures in most of the DRM applications [1–4]. The triangle elements give linear approximation of the surface and they are qualified to give back constant stress distribution. To increase the precision of the membrane analysis an eight-node curved element is introduced here.

The process described below is based on the eight-node quadrilateral element introduced in the paper of Gosling and Lewis [5]. They described a classical finite element approach for geometric nonlinear membranes. In their paper the form-finding process was focused on.

According to our numerical experiments the geometrically nonlinear finite element method they used, is not accurate enough for deformation calculation on prestressed membranes and the linear system equations are ill-conditioned. They use only the first two members of the Taylor-series for the elongation calculation. It gives 0.5–5% error over 0.01–0.05 in-plain elongation and out-of-plane elongation. This amount of elongation is common in textile membrane structures. The condition number of the system equation was over 9000 at every kind of structures, which indicates that the problem is ill-conditioned.

In this paper a continuum mechanical approach is proposed for the deformation calculation. The deformation tensors are calculated from the relation of the basis vectors

* Corresponding author.
E-mail addresses: dizso@silver.szt.bme.hu (D. Hegyi), sajtos@silver.szt.bme.hu (I. Sajtos), gyorgy_geiszter@qdev.hu (G. Geiszter), hinczkrisztian@yahoo.com (K. Hincz).
URLs: http://www.szt.bme.hu (D. Hegyi), http://www.szt.bme.hu (I. Sajtos), http://www.me.bme.hu (K. Hincz).

0045-7949/$ - see front matter © 2006 Elsevier Ltd. All rights reserved.
doi:10.1016/j.compstruc.2006.08.046

of the initial (deformation-free) state and the basis vectors of the actual state.

1.1. Dynamic relaxation method

The DRM is well described in several papers [1–3,6]. It is a fictitious dynamic analysis. In the case of membrane structures it is used for the so-called form-finding problems and for analyses under life loads. In this paper the membrane analysis problem will be described in detail.

In the DRM fictive mass can be used. The mass can be described in a matrix as in any dynamic analyses. To simplify the calculation a diagonal mass matrix can be used as well. According to the second law of Newton the unbalanced loads accelerate the mass:

$$a_i = \frac{f_i}{m_i} \quad \text{or} \quad \bar{a}_i = \bar{f} \cdot \bar{m}^{-1}, \tag{1}$$

where a_i is the acceleration of the node i, f_i is the unbalanced nodal force of node i and m_i is the mass of the node i. $\bar{a}$ is the vector of the acceleration of the nodes of the structure, $\bar{f}$ is the vector of the unbalanced nodal forces and $\bar{m}^{-1}$ is the inverse of the mass matrix of the structure. In Δt the mass moves with

$$s_i = \dot{s}_i \cdot \Delta t + \frac{\ddot{s}_i \cdot \Delta t^2}{2}, \tag{2}$$

where s_i is the movement of node i, $\dot{s}_i$ is the velocity of node i and $\ddot{s}_i = a_i$. The unbalanced loads, the acceleration and the movement are calculated in discrete time steps.

Two types of damping can be used to approach the equilibrium state. The viscous damping is closer to a real dynamic exercise but it has computation difficulties. The kinetic damping [7] is simpler but the stability depends on the time–mass relation.

The basic equations are the following:

$$f_i^t = m_i \cdot \ddot{s}_i + C_i \cdot \dot{s}_i \tag{3}$$

for viscous damping where C_i is the viscous damping factor. For kinetic damping the energy peaks are considered as

$$\dot{s}_i^t = \dot{s}_i^{t-1} + \ddot{s}_i^t \cdot \Delta t \quad \text{and} \quad \dot{s}_i = 0 \quad \text{if} \quad \sum_{i=0}^{n} m_i \cdot \dot{s}_i^{t-1} > \sum_{i=0}^{n} m_i \cdot \dot{s}_i^t. \tag{4}$$

1.2. The discretised mesh

For numerical analysis a mesh is required to describe the structure. The displacements, velocity, acceleration data are calculated at the nodes of the elements. Usually three-node flat triangle elements are used to approximate the spatial membrane surface. The three-node elements are simple to use for calculating the exact deformations, however, only constant stress distribution can be represented inside the elements. Compared to flat triangle elements a better approximation can be achieved with a curved element for the real geometry of the structure and for the deformations as well as it is shown in Fig. 1. The figure shows one quadrilateral, curved element and eight triangle elements covering the same area.

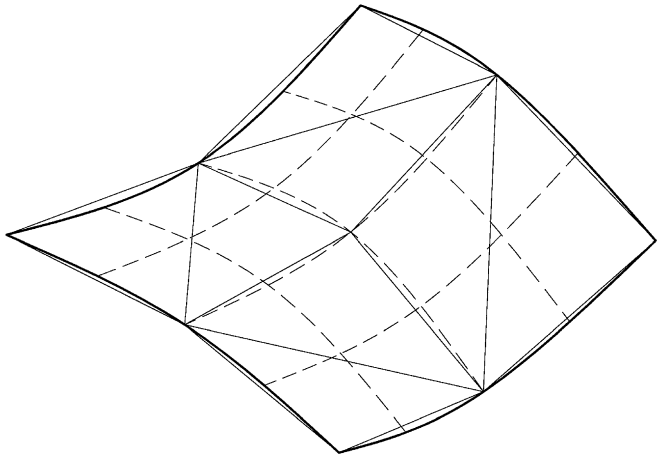

Fig. 1. The three-node and the eight-node elements.

2. The basics of deformation and stress calculation

2.1. The deformation calculation for the eight-node quadrilateral element

During the calculation of the deformations large displacements, large rotations and large strains have to be taken into consideration. A continuum mechanical approach is described here, which can give exact results for any kind of deformation [8–10]. The C^0 shape functions of the eight-node quadrilateral element will be used to approximate the spatial surface of the structure.

The deformations can be calculated between two states of a continuum: the deformation-free state and the actual state (Fig. 2). The deformation-free initial state is described with the so-called Lagrangian coordinates and the actual state with the Euler coordinates.

The deformations are calculated by the relation of the differential line, surface or volume elements. The differential line element is expressed as

$$\mathrm{d}\bar{r}^0 = \frac{\partial \bar{r}^0}{\partial x^{0k}} \mathrm{d}x^{0k}, \tag{5}$$

where $\mathrm{d}r^0$ is the differential line length in the Lagrangian-system, $\bar{r}^0$ is the function of the geometry of the continuum, x^{0k} represent the variables of the coordinate system. (k, l, m and p, q, r are the indices of the coordinate directions in a general basis system; they represent 1, 2, 3.) In the Euler-system we have the same formula:

$$\mathrm{d}\bar{r} = \frac{\partial \bar{r}}{\partial x^p} \mathrm{d}x^p, \tag{6}$$

where $\mathrm{d}r$ is the differential line length in the Euler-system and $\bar{r}$ is the function of the geometry of the continuum.

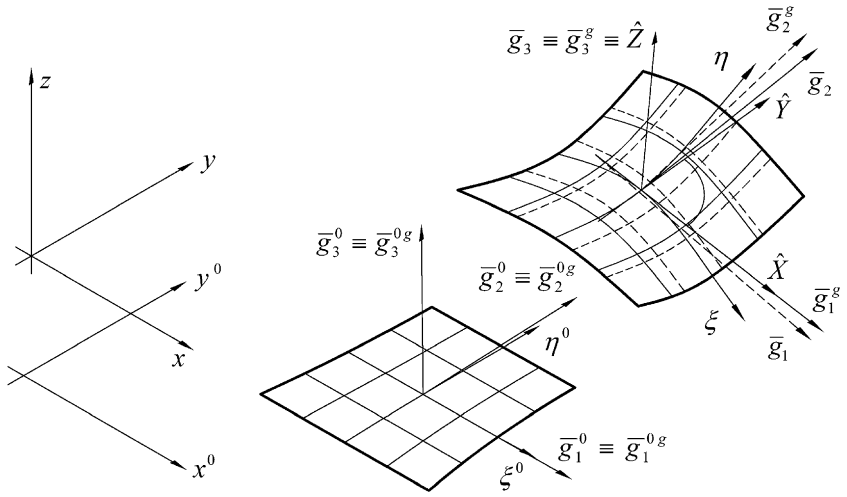

Fig. 2. The basis vectors in the initial and the actual state.

This formula can be expressed with the basis vectors of the different states of the continuum.

$$\bar{g}_k^0 = \frac{\partial \bar{r}^0}{\partial x^{0k}} \quad \text{and} \quad \mathrm{d}\bar{r}^0 = \bar{g}_k^0 \cdot \mathrm{d}x^{0k} \tag{7}$$

$$\bar{g}_p = \frac{\partial \bar{r}}{\partial x^p} \quad \text{and} \quad \mathrm{d}\bar{r} = \bar{g}_p \cdot \mathrm{d}x^p \tag{8}$$

r^0 and r are described with the shape functions of the eight-node quadrilateral element in this paper. The variables are the coordinates of the parametric system:

$$\bar{r}_{(\xi\eta)}^0 = \sum_{i=1}^{8} N_{(\xi\eta)i} \cdot \bar{r}_i^0, \tag{9}$$

$$\bar{r}_{(\xi\eta)} = \sum_{i=1}^{8} N_{(\xi\eta)i} \cdot \bar{r}_i, \tag{10}$$

where $N_{(\xi\eta)i}$ is the shape function for node i, $\bar{r}_i^0$ is the location vector of the nodes in the Lagrangian-system and $\bar{r}_i$ is the location vector in the Euler-system.

According to Ref. [10] the parametric variables can be used in the partial derivation with the parametric infinitesimal length.

$$\bar{g}_k^0 = \frac{\partial \bar{r}^0}{\partial \xi^{0k}} \quad \text{and} \quad \mathrm{d}\bar{r}^0 = \bar{g}_k^0 \cdot \mathrm{d}\xi^{0k}, \tag{11}$$

$$\bar{g}_p = \frac{\partial \bar{r}}{\partial \xi^p} \quad \text{and} \quad \mathrm{d}\bar{r} = \bar{g}_k \cdot \mathrm{d}\xi^k. \tag{12}$$

The transformation between the two states is described by the deformation gradient. This tensor makes a connection between the two states. From the Lagrangian-system to the Euler-system the deformation gradient is the following:

$$\overline{\overline{F}} = \bar{g}_p \circ \bar{g}^{0k}. \tag{13}$$

The basis vectors and the metric tensors determine the geometric state of the continuum. The metric tensors can be written as

$$g_{kl}^0 = \bar{g}_k^0 \circ \bar{g}_l^0, \tag{14}$$

$$g_{pq} = \bar{g}_p \circ \bar{g}_q. \tag{15}$$

There are four basic deformation tensors. Two of them are shown here, both in the Lagrangian-system. First, the Green-deformation tensor gives back the transformation of the initial metric tensor to the actual metric tensor:

$$\bar{g}_p = \overline{\overline{F}} \cdot \bar{g}_k^0, \tag{16}$$

$$g_{pq} = \bar{g}_k^0 \cdot \overline{\overline{F}}^{\mathrm{T}} \cdot \overline{\overline{F}} \cdot \bar{g}_l^0 = \bar{g}_k^0 \cdot \overline{\overline{C}} \cdot \bar{g}_l^0, \tag{17}$$

where $\overline{\overline{C}} = \overline{\overline{F}}^{\mathrm{T}} \cdot \overline{\overline{F}}$ is the Green-deformation tensor. Secondly the difference of the scalar product of the differential line elements gives another deformation tensor:

$$\begin{aligned} \mathrm{d}r_{\mathrm{I}} \cdot \mathrm{d}r_{\mathrm{II}} - \mathrm{d}r_{\mathrm{I}}^0 \cdot \mathrm{d}r_{\mathrm{II}}^0 &= \mathrm{d}r_{\mathrm{I}}^0 \cdot \overline{\overline{F}}^{\mathrm{T}} \cdot \overline{\overline{F}} \cdot \mathrm{d}r_{\mathrm{II}}^0 - \mathrm{d}r_{\mathrm{I}}^0 \cdot \mathrm{d}r_{\mathrm{II}}^0 \\ &= \mathrm{d}r_{\mathrm{I}}^0 \cdot (\overline{\overline{F}}^{\mathrm{T}} \cdot \overline{\overline{F}} - \overline{\overline{I}}) \cdot \mathrm{d}r_{\mathrm{II}}^0 \\ &= \mathrm{d}r_{\mathrm{I}}^0 \cdot 2\overline{\overline{H}} \cdot \mathrm{d}r_{\mathrm{II}}^0, \end{aligned} \tag{18}$$

where $\overline{\overline{H}} = \frac{1}{2}(\overline{\overline{F}}^{\mathrm{T}} \cdot \overline{\overline{F}} - \overline{\overline{I}}) = \frac{1}{2}(\overline{\overline{C}} - \overline{\overline{I}})$ is the Lagrangian-deformation tensor ($\overline{\overline{I}}$ is the unit tensor).

In the Euler-system the inverses of these deformation tensors can be expressed.

The members of the Green-deformation tensor ($\overline{\overline{C}}$) contain the square of the ratio of the original and actual line length. The members of the Lagrangian-deformation tensor ($\overline{\overline{H}}$) contain the half of the difference of the square of the ratio of the original and actual line length and the unit tensor elements. If the strain is small, the elements of the Lagrangian-deformation tensor give back good approximation for the stretch (elongation) and the angle distortions of the continuum. In that case the Euler- and the Lagrangian-deformations are almost identical. If the elongations are not small, the line element stretch and the angle distortion are the following:

$$\varepsilon_e = \frac{\mathrm{d}s}{\mathrm{d}s^0} - 1 = \sqrt{C_{kl} e^{0k} e^{0l}} - 1, \tag{19}$$

where ε_e is the stretch in the direction of $\bar{e}$, e^{0k} are the contravariant scalar coordinates of the entity vector of this direction in the Lagrange-coordinate system, ds^0 is the length of the line element in the Lagrange-coordinate system and ds is the length of the line element in the Euler-coordinate system.

The angle distortion can be calculated from the Lagrangian-deformation tensor as

$$\frac{1}{2}\sin\gamma_{\mathrm{I,II}} = \frac{H_{kl}e^{0k}_{\mathrm{I}}e^{0l}_{\mathrm{II}}}{(1+\varepsilon_{\mathrm{I}})(1+\varepsilon_{\mathrm{II}})}, \tag{20}$$

where $\gamma_{\mathrm{I,II}}$ is the angle deformation between the I and II axis, $\bar{e}^0_{\mathrm{I}}$ and $\bar{e}^0_{\mathrm{II}}$ are the identity vectors of the two directions between whom the angle distortion is calculated.

2.2. Calculation of the stresses

The material law of the typical membrane fabric is nonlinear according to the stress–strain relation and the time–elongation relation. However, in this paper these problems are neglected, only the geometric nonlinearity is taken into account, the Hook's low is used.

Normally the elongations are calculated from the ratio of the increase of the length and the initial length:

$$\varepsilon = \frac{l - l^0}{l^0}, \tag{21}$$

where ε is the elongation, l is the actual length, and l^0 is the initial length. The stress is calculated from the actual load divided by the initial area

$$\sigma = \frac{F}{A^0}, \tag{22}$$

where σ is the stress, F is the actual force and A^0 is the initial area of the section.

This description of σ comes from the second Piola–Kirchhoff ($\overline{\overline{S}}$) stress. (The second Piola–Kirchhof stress is the actual stress transformed back to the initial surface with the initial normal direction.)

In practice the material law is given in the fibre directions, therefore it is beneficial, if the elongations are calculated in these directions. Since in the previous section the calculation of the elongation was described, now only the contravariant scalar coordinates of the identity vectors of the fibre directions have to be calculated for Eqs. (19) and (20):

$$e^{0k}_{\mathrm{warp}} = \bar{e}_{\mathrm{warp}} \cdot \bar{g}^{0k}, \tag{23}$$

$$e^{0k}_{\mathrm{weft}} = \bar{e}_{\mathrm{weft}} \cdot \bar{g}^{0k}. \tag{24}$$

Here the vector formalism is used for the stress calculation:

$$\bar{\sigma} = \overline{\overline{E}} \cdot \bar{\varepsilon}, \tag{25}$$

where $\bar{\sigma}$ is the stress in vector format, $\bar{\varepsilon}$ is the deformation in vector format and $\overline{\overline{E}}$ is the material stiffness in matrix format. (Normally the stress and the deformation are symmetric second order tensors and the material law is a symmetric fourth order tensor.) $\bar{\varepsilon}$ vector is filled with the stretches of Eqs. (19) and (20).

Finally the Second Piola–Kirchhoff stress tensor has to be transformed to the actual state which gives the Cauchy-stress tensor ($\overline{\overline{T}}$):

$$\overline{\overline{T}} = \overline{\overline{F}} \cdot \overline{\overline{S}} \cdot \overline{\overline{F}}^{\mathrm{T}} \cdot \frac{1}{|\overline{\overline{F}}|}. \tag{26}$$

3. The coordinate systems and the eight-node quadrilateral curved element

In the previous sections the basis of the calculation of the deformations and the stresses are described. In this section the coordinate systems are collected. The coordinate systems are chosen to fit best the behaviour of the structural tents.

3.1. The global coordinate systems

The design of the tent structures starts with the form-finding process. Equilibrium shape is searched for the designed perimeters with uniform stress distribution. (The uniform stress distribution is the most common requirement.) The result of this process is the theoretical shape.

The theoretical shape is under stress. To get the initial state the deformation- and stress-free state have to be calculated. There are two problems at this point. There is no guarantee for the existence of stress-free and wrinkling-free initial shape for an arbitrary theoretical shape. To solve this problem the spatial double-curved structure is built up of flat patterns of fabric. These patterns cannot give back the exact theoretical shape. There are imperfections because of the orthotropic material law of the material and because of the approximations used during the patterning. (The shape calculated from the cutting pattern with the real material law is the construction shape [3].)

For the initial shape the cutting pattern can be used (Fig. 3). In this way the initial state is flat as the real deformation-free material and the coordinates of the nodes of the cutting pattern can be described in a 2D Cartesian-coordinate system (x^0, y^0). This is the Lagrangian-system. The cutting patterns of the surface are independent at this state. The spatial geometry of the structure and the para-

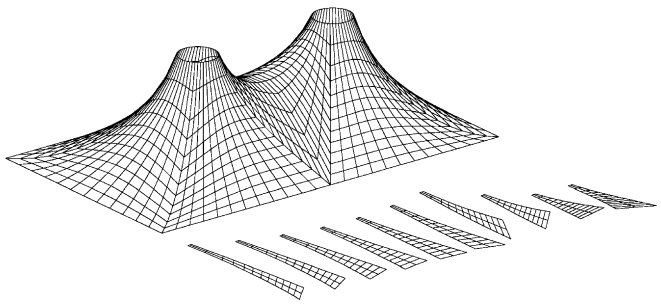

Fig. 3. The 3D structure and the 2D patterns.

metric elements make connections between the slices of the cutting patterns.

An easy way to use the right orthotropic directions is to make the warp and weft direction of the material parallel to the axes of the Lagrangian-coordinate system. In this way the material law can be written in the global coordinate system in the same form for each element.

In the actual state the structure is a spatial surface. The nodes of this structure are described in a 3D Cartesian-coordinate system (x, y, z are the variables).

The Lagrange- and the Euler-coordinate systems can have the same differential length. The x_0, y_0 and x, y axes can be identical. If they are not the same, all the transformations in Section 2.1 need an additional member with the connection of the two coordinate systems. The usage of this transformation can be performed in a smart way to take into consideration the enlargement of the cutting pattern.

3.2. The surface grid coordinate systems

In Section 2 the continuum was an ordinary spatial continuum. In the membrane structures there are two characteristic dimensions and the third dimension can be simplified. The third spatial direction is perpendicular to the surface and the third basis vector is an identity vector. It means that it is enough to use a surface element with two-dimensional parametric coordinates.

There is a parametric coordinate system to describe the geometry within each element and to calculate the basis vectors which fit to the elements at each point ($\bar{g}_1^{0g}, \bar{g}_2^{0g}$, $\bar{g}_3^{0g}$ and $\bar{g}_1^{g}, \bar{g}_2^{g}, \bar{g}_3^{g}$, Fig. 2). For an eight-node quadrilateral surface element the serendipity shape functions can be used for the transformation between the parametric and the global system. The first shape function is

$$N_1 = \frac{(1-\xi)(1-\eta)}{4}(1-\eta-\xi) \tag{27}$$

and the other shape functions can be found in Ref. [11]. These shape functions give linear transformation between the parametric and the global coordinates. It is important to know, that the transformation is linear, if the side nodes are in the middle of the edge. Linear means that the rations in the global and the parametric system are the same. During the deformation the side nodes can move from the middle points, therefore the transformation will not be linear anymore.

The transformation between the parametric system and the global-system has to be linear to get an accurate approximation of the geometry. So in the actual state something more has to be done with the shape functions. Celia and Gray have a paper with such a transformation for eight-node quadrilateral serendipity elements [12]. The first modified shape functions is the following:

$$N_1 = \frac{(1-\xi)(1-\eta)}{4}\left(\frac{(1+\alpha)(1+\varepsilon)-(1+\alpha)(1+\eta)-(1+\varepsilon)(1+\xi)}{(1+\alpha)(1+\varepsilon)}\right) \tag{28}$$

and the other shape functions can be found in the Appendix. α, β, γ, ε are the distances of the side nodes from the middle points in the parametric system.

3.3. The material coordinate systems

In the initial state the material is deformation-free. The distribution of the material is linear through the whole surface. The material coordinates and basis vectors can be identical to the surface coordinates ($\bar{g}_1^0 \equiv \bar{g}_1^{0g}$, $\bar{g}_2^0 \equiv \bar{g}_2^{0g}$, $\bar{g}_3^0 \equiv \bar{g}_3^{0g}$). On the other hand in the actual state the middle points of the eight-node quadrilateral elements move from the middle points of the edges. The nodes belong to the material, so the material coordinate system is not identical to the surface grid coordinate system anymore.

The connection between the grid coordinates and the deformed continuum (the material) can be described with the modified shape functions.

$$\bar{\phi}^m_{(\xi\eta)} = \sum_{i=1}^{8} N_{(\xi\eta)i} \cdot \bar{r}_i^{g-m}, \tag{29}$$

where $\bar{r}_i^{g-m}$ is the distance between node i of the material and the node i of the undeformed parametric element in the parametric grid system. $\bar{\phi}^m_{(\xi\eta)}$ is the function describe the connection of the two system. The corner nodes cannot move from the corners. Only the side nodes are moved with α, β, γ, ε. The material derivatives can be calculated from the grid derivatives with the Jacobian-matrix described with the functional connection following from Eq. (29).

4. The nodal load vector

During the DRM the unbalanced load vector ($\bar{f}$) has to be calculated at each step, as it was written in the first section. The stress calculation is expressed above. The Cauchy-stress tensor has to be reduced to the nodes. The Gauss-integration is used here with the energy principle from the finite element method.

The energy equation is written as

$$\Pi = \frac{1}{2}\int_v (\overline{\overline{L}}\bar{u})^{\mathrm{T}} \cdot \overline{\overline{E}} \cdot (\overline{\overline{L}}\bar{u})\mathrm{d}V - \int_v (\overline{\overline{L}}\bar{u})^{\mathrm{T}} \cdot \overline{\overline{E}} \cdot \varepsilon_0 \,\mathrm{d}V - \int_A \bar{u}^{\mathrm{T}} \cdot \bar{p}_A \,\mathrm{d}A - \int_v \bar{u}^{\mathrm{T}} \cdot \bar{p}_V \,\mathrm{d}V. \tag{30}$$

The displacement function, $\bar{u}$ can be approximated with $\overline{\overline{N}} \cdot \bar{e}$, where $\overline{\overline{N}}$ is the matrix of the shape functions (from Eq. (28)) and $\bar{e}$ is the nodal movement vector. $\overline{\overline{L}}$ is the differential operator matrix. $\overline{\overline{E}} \cdot \bar{\varepsilon}_0 = \sigma_0$ is the initial stress. The first variation of the energy equation, without the work of the stress of the material, gives back the nodal load vector:

$$\bar{q} = \int_v (\overline{\overline{L}}\,\overline{\overline{N}})^{\mathrm{T}} \cdot \sigma_0 \,\mathrm{d}V - \int_A \bar{u}^{\mathrm{T}} \cdot \bar{p}_A \,\mathrm{d}A - \int_v \bar{u}^{\mathrm{T}} \cdot \bar{p}_V \,\mathrm{d}V. \tag{31}$$

The first member can be used to calculate the nodal loads from the internal stresses. The second and third members

are the external surface and volume loads. The first member has to be used to calculate the nodal loads from the internal stress. The stresses have to be calculated at the Gauss-points and multiplied by the deformation matrices ($\overline{\overline{B}} = \overline{\overline{L}}\,\overline{\overline{N}}$) and the weights of the Gauss-points.

The two-dimensional curvilinear parametric system of the surface grid is used to describe the spatial surface of the structure in the 3D global coordinate system. A special formalism is used for the transformations of the deformations between the two systems [5,11]. The nodal movement is described in the 3D global coordinate system. This movement is transformed to the direction of a pair of vectors $\widehat{X}$ and $\widehat{Y}$, as it is also shown in Fig. 2. These vectors are parallel to the surface of the membrane, they are perpendicular to each other, and they have unit length

$$\widehat{u}_{(\xi\eta)} = \begin{bmatrix} \widehat{X}^{\mathrm{T}} \\ \widehat{Y}^{\mathrm{T}} \end{bmatrix} \cdot \begin{bmatrix} N_{(\xi\eta)1} & 0 & 0 & N_{(\xi\eta)2} & 0 & \dots \\ 0 & N_{(\xi\eta)1} & 0 & 0 & N_{(\xi\eta)2} & \dots \\ 0 & 0 & N_{(\xi\eta)1} & 0 & 0 & \dots \end{bmatrix} \cdot \bar{e}_{(x,y,z)}, \tag{32}$$

where $\widehat{u}_{(\xi\eta)}$ is the displacement function vector in the tangential surface coordinate system with parametric variables. To determine the elongation Eq. (32) has to be multiplied by the differential operator:

$$\widehat{\bar{\varepsilon}}^{\widehat{X}\,\widehat{Y}}_{(\xi\eta)} = \overline{\overline{L}} \cdot \widehat{u}_{(\xi\eta)} = \begin{bmatrix} \frac{\partial}{\partial \widehat{X}} & 0 \\ 0 & \frac{\partial}{\partial \widehat{Y}} \\ \frac{\partial}{\partial \widehat{Y}} & \frac{\partial}{\partial \widehat{X}} \end{bmatrix} \begin{bmatrix} u^{\widehat{X}}_{(\xi\eta)} \\ u^{\widehat{Y}}_{(\xi\eta)} \end{bmatrix}. \tag{33}$$

The differential operator is linear, because this deformation is just an infinitesimal deformation to express the nodal loads from the actual stresses for the actual state in one iteration step of the dynamic relaxation.

The variables of the displacement functions are the curvilinear parametric axes. To get the tangent derivatives a special Jacobian-transformation can be used:

$$\begin{bmatrix} \frac{\partial N}{\partial \widehat{X}} \\ \frac{\partial N}{\partial \widehat{Y}} \end{bmatrix} = \frac{1}{|J|} \begin{bmatrix} \bar{g}^g_2 \cdot \widehat{Y} & -\bar{g}^g_1 \cdot \widehat{Y} \\ -\bar{g}^g_2 \cdot \widehat{X} & \bar{g}^g_1 \cdot \widehat{X} \end{bmatrix} \begin{bmatrix} \frac{\partial N}{\partial \xi} \\ \frac{\partial N}{\partial \eta} \end{bmatrix} \tag{34}$$

Finally the elongation vector is the following:

$$\begin{bmatrix} \varepsilon_{\widehat{X}\widehat{X}} \\ \varepsilon_{\widehat{Y}\widehat{Y}} \\ \varepsilon_{\widehat{X}\widehat{Y}} \end{bmatrix} = \frac{1}{|J|} \begin{bmatrix} \widehat{X} \cdot \left(\bar{g}^g_2 \cdot \widehat{Y} \frac{\partial \overline{\overline{N}}}{\partial \xi} - \bar{g}^g_1 \cdot \widehat{Y} \frac{\partial \overline{\overline{N}}}{\partial \eta} \right) \\ \widehat{Y} \cdot \left(-\bar{g}^g_2 \cdot \widehat{X} \frac{\partial \overline{\overline{N}}}{\partial \xi} + \bar{g}^g_1 \cdot \widehat{X} \frac{\partial \overline{\overline{N}}}{\partial \eta} \right) \\ \widehat{Y} \cdot \left(\bar{g}^g_2 \cdot \widehat{Y} \frac{\partial \overline{\overline{N}}}{\partial \xi} - \bar{g}^g_1 \cdot \widehat{Y} \frac{\partial \overline{\overline{N}}}{\partial \eta} \right) + \widehat{X} \cdot \left(-\bar{g}^g_2 \cdot \widehat{X} \frac{\partial \overline{\overline{N}}}{\partial \xi} + \bar{g}^g_1 \cdot \widehat{X} \frac{\partial \overline{\overline{N}}}{\partial \eta} \right) \end{bmatrix} \cdot \bar{e}_{(x,y,z)}. \tag{35}$$

The deformation matrix can be derived from Eq. (35):

$$\overline{\overline{B}} = \frac{1}{|J|} \begin{bmatrix} \widehat{X} \cdot \left(\bar{g}^g_2 \cdot \widehat{Y} \frac{\partial \overline{\overline{N}}}{\partial \xi} - \bar{g}^g_1 \cdot \widehat{Y} \frac{\partial \overline{\overline{N}}}{\partial \eta} \right) \\ \widehat{Y} \cdot \left(-\bar{g}^g_2 \cdot \widehat{X} \frac{\partial \overline{\overline{N}}}{\partial \xi} + \bar{g}^g_1 \cdot \widehat{X} \frac{\partial \overline{\overline{N}}}{\partial \eta} \right) \\ \widehat{Y} \cdot \left(\bar{g}^g_2 \cdot \widehat{Y} \frac{\partial \overline{\overline{N}}}{\partial \xi} - \bar{g}^g_1 \cdot \widehat{Y} \frac{\partial \overline{\overline{N}}}{\partial \eta} \right) + \widehat{X} \cdot \left(-\bar{g}^g_2 \cdot \widehat{X} \frac{\partial \overline{\overline{N}}}{\partial \xi} + \bar{g}^g_1 \cdot \widehat{X} \frac{\partial \overline{\overline{N}}}{\partial \eta} \right) \end{bmatrix} \tag{36}$$

and the unbalanced nodal load is the following:

$$\bar{f} = t \int_A \overline{\overline{B}}^{\mathrm{T}} \cdot \sigma_0 \, \mathrm{d}A. \tag{37}$$

The integration has to be performed on the surface area of the element and t is the thickness of the element.

The positions of the Gauss-points are dictated by the grid parametric coordinate system for accurate integration. The material coordinates for these points can be calculated with the transformations used between the grid and the material system.

5. Example

A simple circular structure is shown in Fig. 4. The structure was analysed with the method described above, with three-node triangle elements and by analytic calculation (only the theoretical shape is worked out analytically). The perimeters, the material properties and the cutting pattern were the same. The radius of the lower circle was 3.0 m, the radius of the higher ring was 1.5 m. The height of the structure was 1.5 m. The lover ring was divided into 24 segments, the upper ring was a circle. There were 24 cutting patterns. There were 96 eight-node quadrilateral elements and different number of triangular elements (from 384 up to 13 824). 4×4 Gauss-points were used in the eight-node analyses.

The form-finding is the first stage of the analysis. It gives back a shape according to the required stress distribution and the perimeters. The result of the form-finding is the theoretical shape. Minimal surface was determined, which means uniform stress distribution over the surface. There was no difference between the three theoretical shapes (the section of the three surfaces is shown in Fig. 5a).

The theoretical shapes were patterned with triangular method. They were shrinked by 2%. The cutting-pattern was stretched back to the edges of the structure. This is the so-called construction-shape with the real stresses of the pre-stressed structure. There was a small difference in the geometry, 3–4 cm (Fig. 5b). The average of the warp and weft stresses was close, but there was big difference in the maximum of the stresses with low number of triangle elements (384) (Table 1). The difference is smaller with higher number of triangle element. The results of the trian-

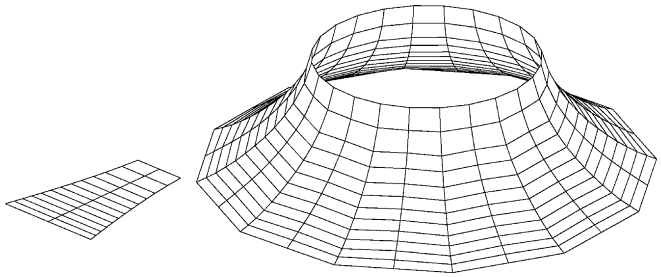

Fig. 4. The circle tent.

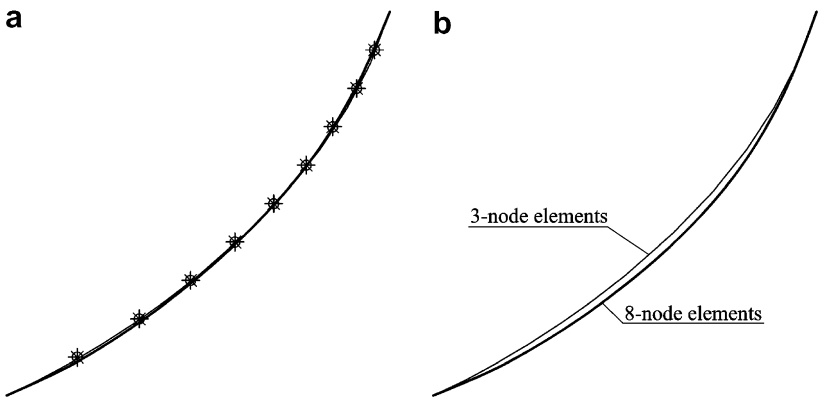

Fig. 5. The geometry of the section of the structure. (a) The theoretical shapes calculated with three-node triangular and eight-node quadrilateral elements and analytically (nodes). (b) The constructional shapes calculated with three-node triangular and eight-node quadrilateral elements.

Table 1
The average and maximum stresses of the construction shape

		Three-node element: 384	Three-node element: 1536	Three-node element: 3456	Three-node element: 6144	Three-node element: 9600	Three-node element: 13824	Eight-node element: 96
Warp direction stresses (kN/cm)	Average	0.017	0.015	0.015	0.015	0.015	0.015	0.021
	Max.	0.017	0.022	0.024	0.026	0.027	0.028	0.035
Weft direction stresses (kN/cm)	Average	0.017	0.016	0.015	0.015	0.015	0.015	0.022
	Max.	0.018	0.023	0.024	0.025	0.025	0.025	0.031

Table 2
The average and maximum stresses of the snow load

		Three-node element: 384	Three-node element: 1536	Three-node element: 3456	Three-node element: 6144	Three-node element: 9600	Three-node element: 13824	Eight-node element: 96
Warp direction stresses (kN/cm)	Average	0.024	0.023	0.023	0.023	0.023	0.023	0.028
	Max.	0.034	0.043	0.048	0.049	0.051	0.052	0.051
Weft direction stresses (kN/cm)	Average	0.014	0.013	0.012	0.012	0.012	0.012	0.018
	Max.	0.023	0.030	0.032	0.033	0.034	0.035	0.032

gle elements converge to the result of the eight-node quadrilateral element (Table 1).

A snow load analysis was performed (1 kN/m^2 distributed load). The experience was the same as with the construction-shape (Table 2).

The main experiences are the following:

- A more complex curved element can give back the local stress peaks around the edges, while the three-node triangle element can give an average stress over one element.
- The average stresses are close to each other. But the eight-node quadrilateral elements provide more detailed results with low number of elements.
- The new method can give better result, but the calculation is much more complex. The usage of the three-node triangle element with few elements was much faster than the usage of the eight-node quadrilateral element, although the eight-node quadrilateral element used less calculation steps. The high number of three-node elements need longer calculation time as the usage of the eight-node elements.

6. Conclusion

A nonlinear continuum mechanical approach was described for the calculation of the nodal force of double-curved membrane elements. This method is suitable to use with the dynamic relaxation method.

The eight-node quadrilateral element can give a better approximation with less number of elements for the geometry of the structure and a more detailed stress distribution than the most commonly used three-node triangle element with DRM.

The described method based on the eight-node quadrilateral element is very robust. However, it requires a large computational effort. In the next steps of the research the

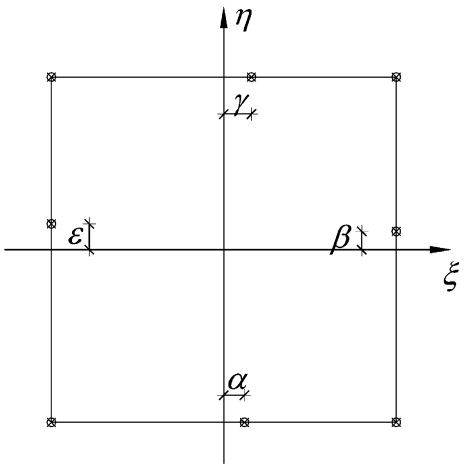

Fig. 6. The improved eight-node element.

benefits of the more accurate element must be weighted by the cost of the calculation time.

Acknowledgement

We would like to thank Peter Iványi for advice in the preparation of this paper.

Appendix

Shape functions of the eight-node improved isoparametric element [12] (Fig. 6):

$$N_1=\frac{(1-\xi)(1-\eta)}{4}\left(\frac{(1+\alpha)(1+\varepsilon)-(1+\alpha)(1+\eta)-(1+\varepsilon)(1+\xi)}{(1+\alpha)(1+\varepsilon)}\right),$$

$$N_2=\frac{1-\eta}{2}\left(\frac{1-\xi^2}{1-\alpha^2}\right),$$

$$N_3=\frac{(1+\xi)(1-\eta)}{4}\left(\frac{(1-\alpha)(1+\beta)-(1-\alpha)(1+\eta)-(1+\beta)(1-\xi)}{(1-\alpha)(1+\beta)}\right),$$

$$N_4=\frac{1+\xi}{2}\left(\frac{1-\eta^2}{1-\beta^2}\right)$$

$$N_5=\frac{(1+\xi)(1+\eta)}{4}\left(\frac{(1-\gamma)(1-\beta)-(1-\gamma)(1-\eta)-(1-\beta)(1-\xi)}{(1-\gamma)(1-\beta)}\right),$$

$$N_6=\frac{1+\eta}{2}\left(\frac{1-\xi^2}{1-\gamma^2}\right),$$

$$N_7=\frac{(1-\xi)(1+\eta)}{4}\left(\frac{(1+\gamma)(1-\varepsilon)-(1+\gamma)(1-\eta)-(1-\varepsilon)(1+\xi)}{(1+\gamma)(1-\varepsilon)}\right),$$

$$N_8=\frac{1-\xi}{2}\left(\frac{1-\eta^2}{1-\varepsilon^2}\right).$$

References

[1] Topping BHV, Khan AI. Dynamic relaxation analysis and design of engineering structures. Struct Eng Comp Tech Seminar 1993.
[2] Iványi P, Topping BHV. Parallel dynamic relaxation formfinding. In: Papadrakokis M, Topping, editors. Innovative computational methods for structural mechanics. Edinburgh: Saxe-Coburg Publications; 1999. p. 124–47.
[3] Gáspár Zs, Hincz K. Formfinding and static analysis of tents. In: IASS Symp Nagoya 2001. TPO42.
[4] Hincz K. Determination of the cutting patterns of prestressed tent structures. Rev Port Eng Est 2000;47:45–9.
[5] Gosling PD, Lewis WJ. Optimal structural membranes—I. Formulation of a curved quadrilateral element for surface definition. Comp Struct 1996;61:871–83.
[6] Day AS. An introduction to dynamic relaxation. The Engineer 1965;219:218–21.
[7] Cundall PA. Explicit finite-difference methods in geometrics. Proc E F Conf Numer Met Gem. Blacksburg; 1976.
[8] Béda Gy, Kozák I, Verhás J. Kontinuummechanika. Budapest: Műszaki Könyvkiadó; 1986.
[9] Kozák I, Pácelt I, Szeidl Gy. Relative motion of continua with applications to the analysis of nonlinear problems by the finite element method. Comput Math Appl 1996;31:191–9.
[10] Basar Y, Weichert D. Nonlinear continuum mechanics of solids. Berlin: Springer; 2000.
[11] Irons B, Ahmad S. Techniques of finite elements. Chichester: Ellis Horwood; 1980.
[12] Celia MA, Gray WG. An improved isoparametric transformation for finite element analysis. Int J Numer Met Eng 1984;20:1443–59.